Catalysis Science & Technology

Accepted Manuscript

ROYAL SOCIETY OF CHEMISTRY

www.rsc.org/catalysis

Optimisation of preparation method for Pd doped Cu/Al_2O_3 catalysts for selective acetylene hydrogenation

Alan J. McCue[1]*, Ashley M. Shepherd[2] and James A. Anderson[1,3]*

[1]Surface Chemistry and Catalysis Group, Department of Chemistry, University of Aberdeen, Aberdeen, UK, AB24 3UE

[2]Chemistry Research Laboratory, University of Oxford, Oxford, UK, OX1 3TA

[2]Materials and Chemical Engineering Group, School of Engineering, University of Aberdeen, Aberdeen, UK, AB24 3UE

Fax: +44 1224 272901, Tel: +44 1224 272905, Email: a.mccue@abdn.ac.uk, j.anderson@abdn.ac.uk

Abstract

Pd doped Cu catalysts have been prepared by co-impregnation, sequential impregnation and a colloidal approach. In each case, the Cu:Pd ratio was optimised leading to catalyst activity which exceeded that offered by monometallic Cu at low temperature (393 K and below) but with a product selectivity which suggests the reaction is still taking place on a Cu surface (i.e., high ethylene selectivity). Pd is therefore thought to influence hydrogen dissociation rates and enhance spillover onto Cu sites. Catalytic testing under more demanding conditions showed differences between the preparation methods. In general, the most active of the samples appeared to be the least selective and *vice-versa*. Under optimised conditions, 50:1 Cu:Pd ratio prepared by sequential impregnation showed an ethylene selectivity of 80% at 98% conversion at only 353 K. Further testing under competitive conditions suggested good ethylene selectivity could be retained under industrially relevant conditions in the absence of CO.

Keywords

Copper, palladium, acetylene, selective hydrogenation, hydrogen spillover.

1. Introduction

Selective alkyne hydrogenation is a process whereby over-hydrogenation to an alkane is avoided and is of significant interest to both industry and academia. Industrially, alkene streams produced from naphtha cracking contain alkyne impurities which need to be removed to low ppm level if the alkene is to be sellable for polymerisation.[1] If this can be achieved through selective hydrogenation then

there is a financial gain since the impurity is converted to additional alkene.[2] In terms of academia, alkyne and alkene hydrogenation are well studied and represent reactions with some very complex underlying chemistry.[3] There are numerous monometallic catalysts reported which offer high C2 selectivity (i.e., the alkane is not formed in significant quantities) such as Cu,[4,5,6,7] Ni,[8,9,10] Au,[11,12,13,14] and Ag[15,16] but these suffer from other drawbacks such as high activation/operating temperatures or are prone to forming oligomeric species leading to deactivation.

Most current industrial catalysts are based on the use of Pd as the active metal, since it can be both activated and operated at relatively low temperature (<393 K).[2] However, Pd does not inherently offer great C2 selectivity and this has been traditionally attributed to Pd ensemble size[1] and more recently to the role of carbide/hydride phases.[3,17,18,19,20,21,22,23] As such, the addition of Ag/Au is necessary to reduce Pd ensemble size and/or minimise hydride formation.[24] Even with optimised industrial catalysts it is generally necessary to co-feed CO to maximise alkene yield. Whilst the addition of a second metal has minimal impact of the industrial process, the use of CO as a transient poison is complex as the quantity added must be regulated in real time as the catalyst deactivates.

To overcome these challenges, different methodologies have been explored including the use of organic S,[25,26,27,28] N[29] and P[28,30] selectivity modifiers pre-adsorbed onto the catalyst surface. This method shows some promise since it can be applied to Pd catalysts allowing for operation at industrially applicable temperatures. Alternatively, much effort has also gone into developing new bi- and tri-metallic catalyst formulations such as Pd-Ga,[31,32] Ni-Zn,[33] Au-Ni,[34,35] Au-Ag[36] and Cu-Ni-Fe,[37] although metal free CeO_2 shows similar traits.[38,39] Whilst these systems offer improved selectivity they require activation/operation at elevated temperatures which may restrict industrial use.

An additional bimetallic system (Cu-Pd) has attracted attention recently with catalytic performance varying depending on the Cu:Pd atomic ratio. It has been shown that the use of small Cu:Pd ratios can produce either supported metal nanoparticles or unsupported alloys which offer enhanced alkene selectivity with Cu acting as a structural diluent.[40,41] The use of high Cu:Pd ratios produce catalysts which combine the intrinsic catalytic properties of Cu (high C2 selectivity) and Pd (active at low-moderate temperature).[42] Based on surface science studies it appears that Pd acts as a site for hydrogen dissociation with hydrogen adatoms spilling over onto neighbouring Cu sites where alkyne hydrogenation occurs.[43,44,45] These findings have been supported by a recent DFT study,[46] although the nature of the Pd site responsible for hydrogen dissociation remains unclear. Such a system represents a potential improvement when compared with other bimetallic formulations since Cu-Pd

catalysts can be activated/operated at relatively low temperatures. In addition, it offers a route to reduce catalyst costs since only small quantities of Pd are necessary and Cu is readily available.

In this study, the catalytic properties of Cu-Pd catalysts prepared from 3 different synthetic routes are compared as well as reporting catalytic performance under industrially relevant conditions (i.e., with alkene present in the feed stream and at elevated pressure). As with a previous report,[42] catalytic conditions have been chosen to achieve high conversion (>99% where possible) which makes the extraction of kinetic parameters of little value since the reaction rate may be mass transfer limited. These conditions do however, represent challenging conditions to retain high C2 selectivity and also mirror the true industrial process where the alkyne concentration must be reduced to low ppm level.

2. Experimental

2.1 Catalyst Preparation

Three series of 10% Cu/Al_2O_3 catalysts modified with varying quantities of Pd were prepared by different methodologies – sequential impregnation, co-impregnation and a colloidal route. Monometallic 10% Cu/Al_2O_3 and 1.67% Pd/Al_2O_3 catalysts were prepared by wetness impregnation as previously reported.[42] All materials were prepared using the same Al_2O_3 support (Aeroxide-Alu C, Evonik, 100 $m^2\ g^{-1}$).

2.1.1 Preparation by sequential impregnation

10% Cu/Al_2O_3 was prepared by impregnation from an aqueous solution of $Cu(NO_3)_2$, followed by drying at 393 K and calcination at 673 K for 3 h in a 100 ml min^{-1} flow. Subsequently, an appropriate volume of an aqueous $Pd(NO_3)_2$ solution (4.3 x 10^{-3} M) was diluted to 100 ml and 2 g of the calcined 10% Cu/Al_2O_3 material added. The mixture was stirred vigorously for 1 h before drying at 393 K and calcination at 673 K for 1 h in a 100 ml min^{-1} flow. Results from our previous study[42] highlight that a 50:1 Cu:Pd ratio results in a catalyst with optimum performance, although reports for a single sample with a 10:1 ratio are shown here for comparative purpose. Samples are denoted as 'X-SI' to signify the metal ratio and preparation method.

2.1.2 Preparation by co-impregnation

Cu (1.3 x 10^{-1} M) and Pd (4.3 x 10^{-3} M) stock solutions were prepared from $Cu(NO_3)_2$ and $Pd(NO_3)_2$, respectively using distilled water. A mixed metal solution was prepared from 25 ml of the Cu stock solution (10 wt% Cu loading) and an appropriate volume of the Pd stock solution and the total volume diluted to 100 ml before Al_2O_3 was added. The mixture was stirred vigorously for 1 h before

drying at 393 K and calcination at 673 K for 1 h in a 100 ml min^{-1} flow. Samples were prepared with 10:1 and 50:1 Cu:Pd ratios and are denoted as 'X-CI' to signify the metal ratio and preparation method.

2.1.3 Preparation by formation of a colloidal preparation

A Cu solution was prepared from $Cu(NO_3)_2$ (0.76 g dissolved in 100 ml distilled water, 10 wt% Cu loading) and mixed with a sodium citrate solution (0.280 g dissolved in 25 ml distilled water) for a period of 10 min. Afterwards, a solution of pre-chilled sodium borohydride (0.150 g dissolved in 20 ml distilled water, 1.25 eq. relative to Cu) was added in 1 portion followed by stirring for 5 min. This resulted in a rapid colour change from blue to black. Next, stirring was continued while a solution of $Pd(NO_3)_2$ was added drop-wise over a period of 20 min. After complete addition of Pd, an acidic slurry of alumina (1.80 g Al_2O_3, 50 ml distilled water, 5 drops of 70% HNO_3) was added. After stirring for 2 h, the solid was filtered, washed (200 ml distilled water), dried at 393 K and calcined at 673 K for 3 h in a 100 ml min^{-1} flow. Samples were prepared with 10:1 and 50:1 Cu:Pd ratio and are denoted as 'X-CP' to signify the metal ratio and preparation method.

2.2 Characterisation

X-ray diffraction patterns of calcined samples were measured in the range of 2θ = 20-60° using an X'Pert powder diffractometer (PANalytical) fitted with a PIXcel1D detector, using Cu Kα radiation and a step size of 0.03° (≈ 10 min acquisition time). The metal oxide crystallite size was estimated by application of the Scherrer equation.

XP spectra of calcined samples were collected using a VG Escalab II spectrometer using Aluminium Kα radiation (1486.6 eV) and a hemispherical analyser for detection of electrons. The Pass Energy was set at 50 eV for survey scan of the sample, and 20 eV for the more intense scans of specific areas. The resulting spectra were analysed using CasaXPS peak fitting software, and sample charging corrected using the C 1s signal at 285.0 eV as reference. Samples were also analysed after reduction and passivation to determine how the surface composition changed during reduction. In this case samples were reduced at 523 K (1:1 H_2:N_2) before cooling to room temperature in nitrogen and storage in air.

Temperature programmed reduction (TPR) experiments were conducted using a TPDRO 1100 instrument with a TCD detector. Profiles were collected in a temperature range of 313-873 K using a heating rate of 5 K min^{-1}. Results are presented per gram of sample and hydrogen consumption quantified based on a response factor determined using a CuO standard.

FTIR of adsorbed CO was performed using a PE Spectrum 100 FTIR spectrometer using an MCT detector with sample presented as a 16 mm diameter self-supporting disc. The disc was suspended in a quartz holder and held in a vacuum line which permitted *in situ* evacuation and gas manipulation. Sample was first heated and reduced in 100 ml min^{-1} of H_2 for 1 h at 523 K (1.67% Pd/Al_2O_3 at 323 K). The sample cell was cooled and evacuated to a pressure of *ca.* $4x10^{-5}$ mbar. An initial spectrum (25 scans, 4 cm^{-1} resolution) was collected prior to stepwise introduction of increasing CO overpressures (0.1-40 Torr). Results are presented as difference spectra relative to the initial scan collected prior to exposure to CO.

2.3 Catalytic tests

Catalyst testing using acetylene as reagent was deliberately conducted under conditions where high conversion (>99%) was generally achieved. Under these conditions it is not appropriate to determine kinetic parameters (i.e., the rate is limited by reagent availability) and as such catalyst activity is only accessed in terms of the minimum temperature required to achieve high conversion. The benefit of working at high conversion is that it represents excellent conditions to access selectivity for a consecutive reaction (i.e., at high conversion it is immediately apparent if a catalyst is prone to converting ethylene into ethane). It should be noted that these conditions also show relevance to the industrial process where high conversion (>99.95%) is a typical requirement.

All catalyst testing was performed in a Microactivity reference reactor (PID Eng & Tech, supplied by Micromeritics) using 100 mg sample diluted with 400 mg SiC located in a 9 mm stainless steel reactor. Prior to reaction, samples were reduced in 30% H_2/N_2 for 1 h at 523 K (1.67% Pd/Al_2O_3 at 323 K). Analysis of the effluent gas was performed using a PE Clarus 580 GC fitted with an FID and a 30 m x 0.53 mm elite alumina capillary column. Acetylene conversion was calculated as the amount reacted divided by the amount introduced. Selectivity to ethylene and ethane was calculated as the amount formed divided by the amount of acetylene reacted. Selectivity to oligomers was calculated based on a carbon balance. In general, catalytic data is presented either as a time on stream (TOS) plot or after 5 h TOS once activity/selectivity appeared constant.

Non-competitive reactions (i.e., no alkene in the feed) were performed with a mixture of 0.6% acetylene/99.4% N_2, with H_2 co-feed to give a H_2:acetylene ratio of either 3:1 or 10:1 at a GHSV of 24000 h^{-1}. Temperature (323-423 K) and pressure (1-5 bar) were varied in separate catalytic tests. Competitive reactions were performed with a mixture of 0.6% acetylene/5.4% ethylene/94% N_2, with H_2 co-feed to give a H_2:acetylene ratio of either 3:1 or 1.5:1 at a GHSV of 24000 h^{-1}.

3. Results

3.1 Synthesis and catalyst screening

Previous study highlighted that CuPd bimetallics which offer enhanced activity (relative to monometallic Cu) whilst maintaining good alkene selectivity could be prepared by a sequential impregnation method.[42] However, the catalytic properties were strongly dependent on the Cu:Pd ratio. In order to access the impact of the preparation method, materials with different Cu:Pd ratio were prepared by co-impregnation, sequential impregnation and a colloidal route. To identify the optimum Cu:Pd ratio for each method, catalyst screening was performed at 373 K to access activity/selectivity for acetylene hydrogenation. This temperature was deliberately chosen since it represents a point where Pd should be very active but unselective, whereas Cu should be moderately active yet show reasonable ethylene selectivity (compare 1.67% Pd/Al_2O_3 and 10% Cu/Al_2O_3 in Table 1). On this basis, 10-SI and 10-CP show high activity but poor ethylene selectivity and represent catalyst formulations where the catalysis is likely dominated by adsorption and reaction on Pd sites or sites strongly influenced by Pd (Table 1). 50-CI fails to demonstrate any enhanced activity relative to monometallic Cu and it is assumed this is because the Pd concentration is too low to influence hydrogen dissociation at 373 K. On the contrary, 10-CI, 50-SI and 50-CP all show higher conversion than 10% Cu/Al_2O_3, yet produce product selectivity which suggests that the reaction is primarily taking place on a Cu surface and therefore represent optimised Cu:Pd ratios for the different preparation routes. Based on the results of these screening tests, the remainder of the results presented will focus on the characterisation of these 3 samples and further catalyst testing, including testing under more industrially relevant conditions.

3.2 Characterisation

XRD measurements were collected using samples in there calcined state. XRD patterns of the 3 samples show peaks at similar 2θ positions, although the peak intensity varies (Figure 1). The majority of the broad signals are attributed to the amorphous Al_2O_3 support used (2θ = 32.8, 34.6, 36.7, 45.5 and 46.5°). In all cases, the Cu metal loading is high enough to be able to identify peaks associated with CuO which are present at 2θ = 35.5, 38.7, 48.8, 53.4 and 58.3°. It should be noted that the CuO reference pattern shows additional weaker peaks at 35.4 and 38.9° 2θ however, these are not apparent in samples discussed here. By application of the Scherrer equation the CuO crystallite size can be estimated as shown in Table 2. The crystallite size for 50-CP is tentatively estimated as <10 nm given that the FWHM cannot be readily distinguished from the broad peaks associated with the support. There is no evidence of PdO crystallites since there are no peaks present in positions typical of PdO (2θ = 33.6, 33.8, 41.9 and 54.7°). This may either because the

loading of Pd is too low to observe by XRD (1.67 wt% for 10-CI and 0.33 wt% for 50-SI and 50-CP), or the Pd is present as a mixed oxide phase with Cu.

XP spectra collected on calcined samples are shown in Figure 2. All 3 samples exhibit a well-defined Cu $2p_{3/2}$ peak between 933-935 eV along with a satellite peak between 942-944 eV suggesting the presence of CuO in agreement with XRD results.[47] 50-SI and 50-CP both exhibit signals associated with PdO (Pd $3d_{5/2}$ ≈337 eV and Pd $3d_{3/2}$ ≈342 eV), however it should be noted that the intensity of the signals are weak, most notably for 50-CP. Curiously, 10-CI does not show any peaks associated with Pd despite the fact that this sample contains the highest nominal Pd loading. This would suggest the absence of a discrete PdO phase but the presence of a mixed oxide phase. It is postulated that co-impregnation is more likely to result in Pd in the bulk of the crystallite since both metals are introduced simultaneously. Given that XPS is a surface sensitive technique and that the metal crystallite size for 10-CI is quite large (≈ 20 nm) it is possible that very little, if any Pd exists close enough to be surface to be detected by XPS (i.e., the concentration is below the limit of detection). Regardless, this result is unexpected and is considered as somewhat unusual. The Cu:Pd ratio for 50-SI and 50-CP in calcined state were calculated by integration of the Cu $2p_{3/2}$ and Pd $3d_{5/2}$ signals and are given in Table 2. The Cu:Pd ratio for 50-CP was calculated as 41 which is similar to the nominal ratio and would suggest that Pd is dispersed relatively uniformly on the surface. In contrast, 50-SI has a calculated Cu:Pd ratio of 13 which is higher than the nominal ratio and indicates that the surface is essentially Pd rich. This may be because during sequential impregnation Pd is preferentially incorporated into the surface layers of CuO particles.

The surface composition and distribution over the support is likely to change following sample reduction and in order to investigate this, samples were pre-reduced under the same conditions used prior to catalytic testing and cooled in nitrogen before being stored in air. Whilst this is likely to result in surface re-oxidation, XPS analysis should reveal a more accurate picture of component distribution over the surface under reaction conditions. After reduction and passivation (data not shown) 10-CI and 50-CP still show a well-defined Cu $2p_{3/2}$ peak with a satellite peak at approximately 943 eV, suggesting that sample re-oxidation resulted in the formation of CuO as opposed Cu_2O. 50-SI sample exhibited a Cu $2p_{3/2}$ peak at 933 eV and a much weaker satellite peak at 943 eV, likely implying a mixture of Cu oxidation states. For all 3 samples, no peaks associated with PdO or Pd were observed and as a result no Cu:Pd ratio could be calculated. This can be, in part, rationalised by considering the lower enthalpy of sublimation of Cu when compared with Pd. As a result it is expected that reduction should result in a surface enriched in Cu and a metal core enriched by Pd.[48,49]

TPR profiles of the 3 samples of interest are displayed in Figure 3 along with a TPR of 10% Cu/Al_2O_3 for reference. Monometallic Cu shows two reduction features at 464 and 507 K which are typical of the two step reduction of CuO to Cu *via* Cu_2O. The integrated peak areas of the first and second peaks are not equal which could imply that the copper in the sample exists in a mixture of oxidation states (i.e., Cu^{2+} and Cu^{+}). However, quantification of the hydrogen consumed suggests complete reduction (based on hydrogen consumed for CuO to Cu based on nominal copper loading), As such it is likely that some CuO is either directly reduced in one step and/or that some of the initial CuO is reduced in an unresolved 2 step reduction process. There are notable differences between the different bimetallic samples. 10-CI exhibits two low temperature reduction features at 372 and 386 K. The first of these is attributed to the reduction of PdO with the second associated with reduction of a mixed oxide phase.[42] Further peaks at 466 and 495 K are thought to be associated with the two step reduction of CuO, although the fact that the second step occurs at a lower temperature than for monometallic Cu indicates that hydrogen dissociation is a more facile process on the bimetallic surface. Similar features are present in 50-SI samples, although the low temperature peak associated with PdO reduction is significantly smaller which is consistent with the reduced Pd loading. The peak positions for CuO reduction do not show a shift towards lower temperature suggesting that hydrogen dissociation occurs less readily on 50-SI than 10-CI which is consistent with catalyst activity (see later). Interestingly, 50-CP shows no distinct peak which can be attributed to reduction of PdO but does show a marked decrease in the temperature necessary to reduce CuO (420 K) and Cu_2O (459 K). The final point of note from the TPR profiles is that none of the bimetallic samples exhibit a negative feature at low temperature indicative of palladium hydride decomposition which indicates that no/very few solely monometallic Pd particles exist. This is important given that palladium hydride is often associated with unselective alkyne hydrogenation.[3,17,18,19,20]

Combined use of FTIR and CO adsorption allowed evaluation of the surface state after reduction at 523 K which mirrors the activation step necessary prior to catalytic testing. Figure 4 shows typical spectra of the two monometallic catalysts (Figure 4-a and c) and a physical mixture of the two monometallic catalysts (Figure 4-b). Reduced 10% Cu/Al_2O_3 exhibits a strong band which is in fact a doublet centred at *ca.* 2110 and 2100 cm^{-1} corresponding to CO linearly adsorbed on Cu^{+} and Cu, respectively.[50] 1.67% Pd/Al_2O_3 reduced at 323 K displays a larger number of bands since CO can adsorb in a number of ways. Bands at 2117, 2095 and 2077 cm^{-1} are assigned to CO linearly adsorbed on Pd cations, Pd-edge sites and Pd-terraces, respectively. Adsorption modes at 1973 and 1930 cm^{-1} correspond to bridging CO and 1878 cm^{-1} to CO bound to 3 fold-hollow sites (Note: gas phase CO bands appear centred at 2143 cm^{-1}). Figure 4-b shows CO adsorbed on a physical mixture

corresponding to a Cu:Pd ratio of 10:1 made up from the two monometallic catalysts. This demonstrates how the spectrum might appear when both metals are present as separate monometallic particles and confirms that the technique is sufficiently sensitive to observe CO adsorption on Pd in a large excess of Cu should the Pd be exposed at the surface. The spectra of the 3 bimetallic catalysts (Figure 4-d to e) are all alike in appearance and look similar to that of 10% Cu/Al_2O_3 with two bands apparent at 2111 and 2101 cm^{-1}. Given that these peaks correspond to CO adsorbed on Cu and Cu^+, all 3 samples appear to have a surface which is dominated by Cu sites which is consistent with XPS analysis after reduction. Importantly, the absence of bridging or 3 fold-hollow Pd sites confirms the absence of any pronounced islands of Pd which would be likely to act as unselective hydrogenation sites (see inserts in Figure 4-d to e).

3.3 Catalytic results

Whilst the true industrial process operates with a large excess of ethylene present in the feed stream relative to acetylene and at higher pressure, simple single reagent reactions proved an efficient means to differentiate between the 3 catalysts characterised in this study. Figure 5 displays acetylene conversion and product selectivity using 3 equivalents of H_2 relative to acetylene in the temperature range 343-373 K after 5 h time on stream. In terms of activity, it is clear that 10-CI is the most active catalyst since close to complete conversion (98.4%) can be achieved at only 343 K. This represents a significant decrease in temperature necessary to achieve high conversion when compared with monometallic Cu (Table 1). 50-CP is the next most active catalyst with 77.4% conversion achieved at 343 K, whereas 50-SI only shows 14.8% conversion at 343 K. As such, the general activity trend can be summarised as 10-CI > 50-CP > 50-SI and this order holds true for all catalytic measurements reported here. Of course, high activity at low temperature is only of benefit if the corresponding product distribution favours ethylene as opposed to ethane. For all 3 catalysts, the major product observed is ethylene with selectivity of 60-75% matching or even surpassing that of pure Cu (≈70% at full conversion).[42] The largest difference between the 3 catalysts is in the selectivity towards over-hydrogenation and oligomer formation. In general, Cu produces significant quantities of acetylene based oligomers, most notably under conditions where hydrogen dissociation is limited. It is therefore not surprising that the catalyst which is least active (50-SI) exhibits the highest selectivity to oligomers, although this decreases at 373 K once full conversion is reached. Both 10-CI and 50-CP tend to produce fewer oligomers, however, do produce more ethane than 50-SI as temperature is increased.

The next set of tests used to distinguish between samples was to operate with a 10 fold excess of hydrogen relative to acetylene (Figure 6). The first consequence of operating under these conditions

is that higher conversion can be achieved at even lower temperatures. For example, full acetylene conversion is observed over 10-CI at 323 K with 10 eq. H_2 compared with 353 K with 3 eq. H_2. Similar trends can be found concerning 50-SI and 50-CP. Clear differences in product selectivity are apparent with 10-CI producing ethane as the pre-dominant product (65-87% selectivity), highlighting that high activity is not necessarily beneficial for achieving high alkene selectivity. 50-CP exhibits high ethylene selectivity at 323 and 333 K, however, increasing the temperature further increases ethane selectivity until ethylene and ethane are almost produced in a 1:1 ratio at 353 K. The most promising catalyst under these more demanding conditions is clearly 50-SI, although only 98% conversion is achieved at 353 K. As temperature is increased, ethane selectivity remains low (< 10%) and oligomer selectivity even drops at the expense of enhanced ethylene selectivity (80%). The trend in selectivity (50-SI > 50-CP > 10-CI) appears to be the reverse of the trend in activity (10-CI > 50-CP > 50- SI). On the basis of this set of data, 10-CI and 50-CP samples were disregarded from further experiments.

Industrially, olefin purification is typically performed under moderate pressure. In order to access selectivity as a function of pressure, a test with 50-SI was performed in the range 1-5 bar, (note: industrial operating pressure generally exceeds the 5 bar limit used here) and at a fixed temperature (373 K) where 100% acetylene conversion was expected based on earlier tests. A time on stream plot for 50-SI is shown in Figure 7 and demonstrates fairly stable activity/selectivity over a 5 h period. As pressure increases, ethylene selectivity decreases, primarily as a result of more over-hydrogenation. At 5 bar pressure, ethylene selectivity drops to 59% with ethane and oligomer selectivity reaching 22 and 19%, respectively. This suggests that whilst 50-SI sample exhibits high activity and selectivity at low pressure, it may not be suited to working at higher pressures.

A final test reaction was performed with ethylene added to the feed gas to examine selectivity under competitive conditions (Figure 8). Reactions were performed at 1 bar pressure in order to work under optimum conditions for 50-SI sample. Note that with a large excess of ethylene present in the feed gas it proved harder to determine oligomer selectivity purely based on carbon balance and as such results are presented in terms of 'C2 product selectivity' since these could be determined with confidence. Under competitive conditions full conversion was harder to achieve using a 1.5:1 H_2:acetylene ratio. At 383 K, 50-SI resulted in 82% conversion and 77% selectivity to ethylene. Increasing the H_2:acetylene ratio to 3:1 allowed for 100% acetylene conversion to be achieved at 363 K but with decreased ethylene selectivity (57%). It should be highlighted that these tests were conducted in the absence of CO which is added industrially to control selectivity.

4. Discussion

4.1 Catalyst design

In order to prepare a CuPd bimetallic catalyst where Cu acts as the primary site for hydrogenation and Pd enhances hydrogen dissociation certain characteristics are desirable. Firstly, large Pd ensembles should be avoided as these would act as sites for unselective hydrogenation. Secondly, Pd should ideally be situated in sites which can influence hydrogen dissociation (presumably in the surface or near surface layers). In principle, both these factors can be controlled by the Cu:Pd ratio and the thermal history of a material. The idea of preparing a catalyst by a sequential impregnation methodology was that Pd can either be deposited onto pre-formed CuO particles, or onto the support in close proximity to these particles. During the subsequent thermal treatment metal mixing would be expected, although ideally with Pd remaining near the surface. Characterisation of 50-SI suggests that there are no monometallic Pd particles present since there is no evidence of CO adsorbing in bridging or threefold hollow sites (Figure 4-e) and no hydride decomposition was detected by TPR (Figure 3-c). Pleasingly, the Cu:Pd atomic ratio of 13 determined by XPS prior to reduction (Table 2) is smaller than the nominal ratio suggesting that the surface layers are essentially Pd rich, consistent with the intended catalyst design. XPS analysis of this sample after reduction suggests that the surface Pd concentration decreases with Pd likely to migrate towards to the centre of bimetallic particles. The last point of note for 50-SI sample is that the TPR profile shows no shift with respect to Cu/Al_2O_3 in terms of the temperature necessary to reduce Cu^{2+} to Cu^0 (Figure 3) suggesting this sample should dissociate hydrogen with the greatest degree of difficulty of the bimetallic samples.

It was postulated that a similar material could be prepared using a solution phase approach. In this case Cu nanoparticles were prepared by reduction of a Cu^{2+} salt using a small excess of $NaBH_4$. The slow addition of a dilute Pd salt solution into the excess reducing agent should result in the formation of Pd^0 in solution which should bind to the existing Cu nanoparticles as opposed to forming separate monometallic Pd nanoparticles as long as the addition of Pd was slow. After the nanoparticles were deposited onto the support they were calcined at the same temperature as 50-SI sample but for a 3 h period. This again appeared to result in a material devoid of monometallic Pd particles based on FTIR of adsorbed CO (Figure 4-f) and TPR (Figure 3-d). The difference in this case is that after calcination a more uniform distribution of Pd over the surface is expected since the Cu:Pd ratio calculated from XPS data is 41 (Table 2). Again, after reduction, XPS suggests that Pd migrates towards the bulk to leave a Cu rich surface. It therefore appears that the properties of 50-CP may not be strongly influenced by the preparation step but rather by the subsequent thermal treatment upon where metal mixing will take place. This sample also displays a different TPR profile

with no peak which can be assigned to reduction of PdO, however does exhibit a significant decrease in the temperature required to reduce CuO and Cu_2O, suggesting that hydrogen dissociation is facilitated on this surface (Figure 3-d).

The final preparation method investigated was co-impregnation where both metals salt are introduced simultaneously which may result in a degree of metal mixing prior to any thermal treatment. Characterisation of this sample also suggests the absence of Pd or PdO particles (see XRD pattern, Figure 1-c), however there appears to be little evidence of Pd being present on the surface of the bimetallic particles (Figure 4-d). This statement is exemplified by the lack of Pd observed by XPS (Figure 2-a) before or after reduction. Prior to reduction, it is possible that the metal particles contain a PdO rich core contained within a CuO rich shell which is too thick to allow for the core to be observed by XPS. As a result, the surface composition of 10-CI is not expected to change as significantly after reduction. The escape distance of an electron from CuO or PdO corresponds to the inelastic mean free path at their binding energy which are estimated as 1.5 and 0.8 nm for Cu and Pd metal, respectively.[51] Given that the particle size of 10-CI is relatively large (Table 2) it is possible that no Pd exists close enough to the particle surface to be detected by XPS. A similar approach has been previously used to interpret XPS data for similar CuPd samples.[45] However, this explanation appears somewhat unsatisfactory given that this sample contains the largest amount of Pd. It also calls into question the mechanism by which this sample exhibits enhanced catalytic activity relative to monometallic Cu (i.e., are Pd surface/near-surface atoms/clusters necessary to dissociate hydrogen). The only evidence of the presence of Pd comes from the TPR profile with new peaks apparent at 373 and 386 K (Figure 3-b). The first of these can be assigned to PdO reduction with the second thought to be related to reduction of a mixed oxide phase. There is only a small shift in the reduction features associated with $Cu_2O \rightarrow Cu$ which is not entirely consistent with the high activity shown by this sample.

4.2 Influence of preparation route on catalyst activity

Catalytic data presented here was (where possible) collected at full conversion. These conditions were considered as beneficial given that they represent challenging conditions to achieve high ethylene selectivity since ethylene hydrogenation is most favourable in the absence of acetylene. As a result, activity is judged purely on the basis of the temperature necessary to achieve as close to full conversion as possible. All 3 samples demonstrate considerably enhanced activity at low temperature (see Table 1, Figure 5 and Figure 6) compared with monometallic Cu (50-80 K decrease to achieve full conversion) and importantly can be operated at temperatures similar to those currently used industrially. There is also no evidence of deactivation over a period of 5 h TOS which

is interesting since Cu catalysts often deactivate during alkyne hydrogenation, most notably at lower temperatures.[4,7,52] The only reported example of a 'Pd free' catalyst which can operate at these temperatures is a Ni-Au catalyst reported by Nikolaev *et al*.[34,35] Regardless of whether tests were conducted with 3 or 10 equivalents of hydrogen relative to acetylene, there is a clear activity trend within the series (10-CI > 50-CP > 50-SI). The opposite trend may have been expected since 50-SI has the lowest Cu:Pd ratio in the surface layers determined by XPS after calcination. This highlights that characterisation of samples prior to reduction may give a false impression of surface composition during reaction conditions. A recent DFT study by Fu and Luo highlights that the energy barrier limiting hydrogen dissociation varies significantly depending on both the number of Pd atoms populating the surface/sub-surface region of a Cu(111) surface and the Pd-Pd atom interconnectivity.[46] Their work suggests that small clusters of Pd which populate the surface and sub-surface layers act as sites with only a small energy barrier limiting hydrogen dissociation.[46] In order to justify why 50-CP is more active than 50-SI the Pd might exist in such clusters. 10-CI is the most active catalyst and this is likely associated with the larger Pd loading and the distribution of the two components. No Pd was detected by XPS after calcination suggesting a structure which had a Pd rich core and a Cu rich surface. To rationalise why 10-CI exhibits such high activity a literature survey was conducted to determine if $Pd_{core}Cu_{shell}$ structures could successfully be synthesised. Procedures exist for the preparation of CuPd nanoparticles with either a Pd[53] or Cu shell,[54] however there is no relevant catalytic data to access the impact on activity suggesting there is scope for future work.

4.3 Influence of preparation route on product selectivity

Monometallic Cu and Pd catalysts show such distinct differences in selectivity that this can be used as an indicator of which acts as the primary site for hydrogenation on bimetallic samples. Under simplified conditions (3:1 H_2:acetylene, non-competitive), all 3 samples demonstrate selectivity consistent with the reaction taking place on a Cu surface (Table 1). There are subtle differences in selectivity which are also indicative of Cu dominated behaviour (Figure 5). Previous reports indicate that the major by-product produced over Cu catalysts are oligomers,[4,7,52] with higher oligomer selectivity apparent under conditions where hydrogen availability is limited. The CuPd catalysts discussed are more active than monometallic Cu which results in decreased oligomer selectivity. The net result is that ethane and/or ethylene selectivity must increase. 10-CI and 50-CP show a considerable decrease in oligomer selectivity (10-20%) with an increase in ethylene and ethane selectivity (≈ 5-10%). Test reactions with a larger excess of hydrogen (Figure 6) suggests that there is a trade-off between high activity and higher ethane selectivity since 10-CI (most active) produces the highest ethane selectivity whereas 50-SI (least active) still displays < 10% to ethane under more

demanding conditions. It is interesting to note that the highest ethylene selectivity produced by 50-SI occurs at the highest test temperature with both 3 and 10 equivalents of H_2. Given that as temperature increases, Cu activity increases, it is possible that the highest selectivity occurs when hydrogen dissociation occurs directly on Cu as well as *via* a spillover mechanism from sites influenced by Pd.

Since 50-SI was the most selective of the 3 catalysts under simple test conditions, this sample was used for testing at higher pressure and under competitive conditions to examine performance under more industrially relevant conditions. Increasing pressure from 1 to 5 bar under conditions which achieve 100% conversion (Figure 7) gradually results in a decrease in ethylene selectivity with an increase in ethane formation. Two explanations for the decrease in selectivity are possible. Firstly, at higher pressures, the enhanced ability of 50-SI to dissociate hydrogen leads to increased over-hydrogenation or secondly, Cu is less selective when operating at higher pressures. Given that the high inherent selectivity of Cu is generally associated with a barrier limiting ethylene adsorption, the later explanation seems less plausible. However, it should be noted that little information regarding alkyne hydrogenation over Cu at high pressure has been reported with studies generally performed at 1 bar pressure.[4,6,7,52] A test performed with 50-SI under competitive conditions indicates that the good ethylene selectivity observed under non-competitive conditions can still be attained with ethylene present as a major component of the feed gas (Figure 8). The combination of activity at low-moderate temperatures and high ethylene selectivity under competitive conditions suggests that Pd promoted Cu catalysts show some promise as an alternative to the current industrial catalysts. The added advantage of retaining good ethylene selectivity in the absence of CO as a competitive adsorbate offers an additional advantage. However, it must be acknowledged that as alkene selectivity appears to decrease as pressure is increased, this would require a marked change in how the industrial process occurs.

5. Conclusions

Pd promoted Cu/Al_2O_3 catalysts were prepared by 3 different synthetic routes and the Cu:Pd ratio optimised for each method. The result was the formation of CuPd catalysts which are significantly more active than monometallic Cu but at temperatures which are of relevance to industrial alkyne hydrogenation. These samples also retain the high alkene selectivity typically observed with monometallic Cu. Testing under conditions with a larger H_2:acetylene ratio highlights that the trend in activity (10-CI > 50-CP > 50-SI) is the opposite regarding selectivity (50-SI > 50-CP > 10-CI) suggesting that a balance between activity and selectivity must be reached. Testing of the most selective catalyst (50-SI) at higher pressure and under competitive conditions suggests that optimum

selectivity is only likely to be obtained at lower pressures, however this selectivity can be retained when reactions are performed with a feed gas containing ethylene.

References

[1] A. Borodzinski and G. C. Bond. *Catal. Rev.*, 2008, **50**, 379.
[2] D. B. Tiedtke, t. T. P. Cheung, J. Leger, S. A. Zisman, J. J. Bergmeister and G. A. Delzer in: *13th Ethlyene Producers Conference*, 2001, **10**, p. 1.
[3] D. Teschner, J. Borsodi, A. Wootsch, Z. Revay, M. Hävecker, A. Knop-Gericke, S. D. Jackson and R. Schlögl. *Science*, 2008, **320**, 86.
[4] B. Bridier, N. López and J. Pérez-Ramírez. *J. Catal*., 2010, **269**, 80.
[5] B. Bridier, M. A. G. Hevia, N. López and J. Pérez-Ramírez. *J. Catal*., 2010, **278**, 167.
[6] J. T. Wehrli, D. J. Thomas, M. S. Wainwright and D. L. Trimm. *Appl. Catal.*, 1990, **66**, 199.
[7] J. T. Wehrli, D. J. Thomas, M. S. Wainwright and D. L. Trimm. *Appl. Catal*., 1991, **70**, 253.
[8] D. L. Trimm, I. O. Y. Liu and N. W. Cant. *Appl. Catal. A: Gen*., 2010, **374**, 58.
[9] D. L. Trimm, N. W. Cant, I. O. Y. Liu. *Catal. Today*, 2011, **178**, 181.
[10] S. Abelló, D. Verboekend, B. Bridier and J. Pérez-Ramírez. *J. Catal.*, 2008, **259**, 85.
[11] T. V. Choudhary, C. Sivadinarayana, A. K. Datye, D. Kumar and D. W. Goodman. *Catal Lett.*, 2003, **86**, 1.
[12] Y. Azizi, C. Petit and V. Pitchon. *J. Catal.*, 2008, **256**, 338.
[13] Y. Segura, N. López and J. Pérez-Ramírez. *J. Catal*., 2007, **247**, 383.
[14] X. Liu, C-Y. Mou, S. Lee, Y. Li, J. Secrest and B. W.-L. Jang. *J. Catal.*, 2012, **285**, 152.
[15] A. Sárkány and Z. Révay. *Appl. Catal. A: Gen*., 2003, **243**, 347.
[16] G. Vilé, D. Baudouin, I. N. Remediakis, C. Copéret, N. López and J. Pérez-Ramírez. *ChemCatChem 2013, **5**, 3750.*
[17] W. Ludwig, A. Savara, K-H. Dosert and S. Shauermann. *J. Catal*., 2011, 284, 148.
[18] W. Ludwig, A. Savara, R. J. Madix, S. Schauermann and H. J. Freund. *J. Phys. Chem. C*., 2012, **116**, 3539
[19] F. Viñes, C. Loschen, F. Illas and K. M. Neyman. *J. Catal*., 2009, **266**, 59.
[20] M. Armbrűster, M. Behrens, F. Cinquini, K. Föttinger, Y. Grin, A. Haghofer, B. Klötzer, A. Knop-Gericke, H. Lorenz, A. Ota, S. Penner, J. Prinz, C. Rameshan, Z. Révay, D. Rosenthal, G. Rupprechter, D. Teschner, D. Torres, R. Wagner, R. Widmer and G. Wowsnick. *ChemCatChem* 2012, **4**, 1048.
[21] J. Sá, G. D. Arteaga, R. D. Daley, J. Bernardi and J. A. Anderson. *J. Phys. Chem. B*, 2006, **110**, 17090.
[22] B. Bridier, N. López and J. Pérez-Ramírez. *Dalton Trans*., 2010, **39**, 8412.
[23] M. García-Mota, B. Bridier, J. Perez-Ramírez and N. López, *J. Catal*. 2010, **273**, 92.
[24] N. A. Khan, S. Shaikhutdinov and H. J. Freund. Catal. Lett., 2005, **108**, 159.
[25] A. J. McCue and J. A. Anderson. *Catal. Sci. Tech*nol., 2014, **4**, 272.
[26] F. M. McKenna and J. A. Anderson. J. Catal., 2011, **281**, 231.
[27] F. M. McKenna, R. P. K. Wells and J. A. Anderson. Chem. Comm., 2011, **47**, 2351.
[28] F. M. McKenna, L. Mantarosie, R. P. K. Wells, C. Hardacre and J. A. Anderson. Catal. Sci. Technol., 2012, **2**, 632.
[29] L. Altmann, X. Wang, J. Stöver, M. Klink, V. Zielasek, K. Thiel, J. Kolny-Olesiak, K. Al-Shamery, H. Borchert, J. Parisi and M. Bãumer. *ChemCatChem* 2013, **3**, 1803.
[30] A. J. McCue, F. M. McKenna and J. A. Anderson. *Catal. Sci. Technol*., 2015, DOI: 10.1039/c5cy00065c.
[31] J. Osswald, R. Giedigkeit, R. E. Jentoft, M. Armbrűster, F. Girgsdies, K. Kovnir, R. Ressler, Y. Grin and R. Schlögl. *J. Catal.*, 2008, **258**, 210.
[32] J. Osswald, K. Kovnir, M. Armbrűster, R. Giedigkeit, R. E. Jentoft, U. Wild, Y. Grin and R. Schlögl. *J. Catal.*, 2008, **258**, 219.
[33] F. Studt, F. Abild-Pedersen, T. Bligaard, R. Z. Sørensen, C. H. Christensen and J. K. Nørskov. *Angew. Chem. Int. Ed*., 2008, **47**, 9299.
[34] S. A. Nikolaev, V. V. Smirnov, A. Yu Vasil'kov and V. L. Podshibikhin. Kinetics and Catalysis, 2010, **51**, 375.
[35] S. A. Nikolaev and V. V. Smirnov. *Catal. Today*, 2009, **147S**, S336.
[36] X. Liu, Y. Li, J. W. Lee, C.-Y. Hong, C.-Y. Mou and B. W. L. Jang. *Appl. Catal. A: Gen*., 2012, **439**, 8.
[37] B. Bridier and J. Pérez-Ramírez. *J. Am. Chem. Soc*., 2010, **132**, 4321.
[38] G. Vilé, B. Bridier, J. Wichert and J. Pérez-Ramírez, *Angew. Chem. Int. Ed*., 2012, **51**, 8620.

[39] J. Carrasco, G. Vilé, D. Fernández-Torre, R. Pérez, J. Pérez-Ramírez and M. V. Ganduglia-Pirovano, *J. Phys. Chem. C*, 2014, **118**, 2014, 5352.
[40] S. K. Kim, J. H. Lee, I. Y. Ahn, W. J. Kim and S. H. Moon. *Appl. Catal. A: Gen*., 2011, **401**, 12.
[41] M. Friedrich, S. A. Villaseca, L. Szentmiklósi, D. Teschner and M. Armbrűster. Materials, 2013, **6**, 2958.
[42] A. J. McCue, C. J. McRitchie, A. M. Shepherd and J. A. Anderson. *J. Catal*., 2014, **319**, 127.
[43] H. L. Tierney, A. E. Baber, J. R. Kitchin and E. C. H. Sykes. Phys. Rev. Lett., 2009, **103**, 246102.
[44] G. Kyriakou, M. B. Boucher, A. D. Jewell, E. A. Lewis, T. J. Lawton, A. E. Baber, H. E. Tierney, M. Flytzani-Stephanopoulos and E. C. H. Sykes. Science, 2012, **335**, 1209.
[45] M. B. Boucher, B. Zugic, G. Cladaras, J. Kammert, M. D. Marchinkowski, T. J. Lawton, E. C. H. Sykes and M. Flytzani-Stephanopoulous, Phys. Chem. Chem. Phys., 2013, **15**, 12187.
[46] Q. Fu and Y. Luo. *ACS Catal*., 2013, **3**, 1245.
[47] J. Bastista, A. Pintar, D. Mardrino, M. Jenko and V. Martin, *Appl. Catal. A: Gen*., 2001, **206**, 113.
[48] M. Fernández-García, J. A. Anderson and G. L. Haller, *J. Phys. Chem*., 1996, **100**, 16247.
[49] M. Fernández-García, A. Martínez-Arias, C. Belver, J. A. Anderson, J. C. Conesa and J. Soria, *J. Catal*., 2000, **190**, 387.
[50] P. Hollins, *Surf. Sci. Rep*, 1992, **16**, 51.
[51] P. J. Cumpson and M. P. Seah, *Surf. Interface Anal.*, 1997, **25**, 430.
[52] N. J. Ossipoff and N. W. Cant, *J. Catal.*, 1994, **148**, 125.
[53] J. Cai, Y. Zeng and Y. Guo, *J. Power Sources*, 2014, **270**, 257.
[54]M. Jin, H. Zhang, J. Wang, X. Zhong, N. Lu, Z. Li, Z. Xie, M. J. Kim and Y. Xia, *ACSNano*, 2012, **6**, 2566.

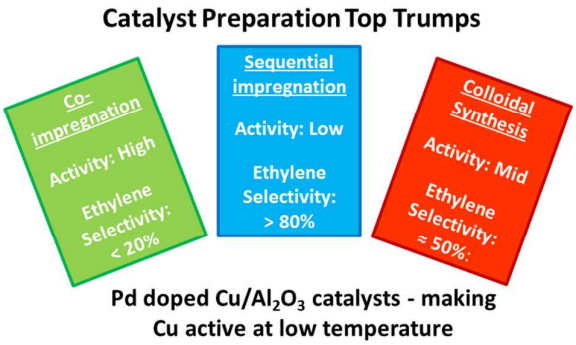

3 preparation methods were explored for preparing CuPd catalysts for selective acetylene hydrogenation leading to materials which were selective and active at lower temperatures than normally observed for Cu catalysts.

Tables

Table 1 – Acetylene conversion and product selectivity from catalyst screening measurements performed at 373 K.

Sample	Acetylene conversion / %	Selectivity / %		
		Ethylene	Ethane	Oligomers
10% Cu/Al_2O_3	61	61	9	30
1.67% Pd/Al_2O_3	100	0	93	7
10-CI	100	68	12	20
50-CI	34	64	2	34
10-SI	100	7	79	14
50-SI	100	71	6	23
10-CP	100	0	93	7
50-CP	100	68	20	12

Table 2 – Nominal metal loading, Cu:Pd atomic ratio and CuO particle size determined by XRD.

Sample	Cu / wt%	Pd / wt%	Cu:Pd atomic ratio	CuO crystallite size from XRD / nm[a]	XPS Cu:Pd atomic ratio from calcined sample
10-CI	10	1.67	10	20	nd
50-SI	10	0.33	50	23	13
50-CP	10	0.33	50	<10	41

[a] Estimated from XRD pattern of calcined sample using the Scherrer equation

Figures

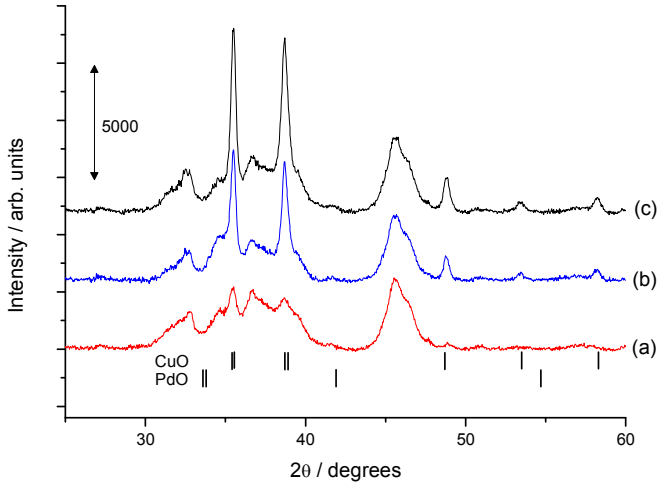

Figure 1 – XRD patterns following calcination but before reduction for (a) 50-CP, (b) 10-CI and (c) 50-SI

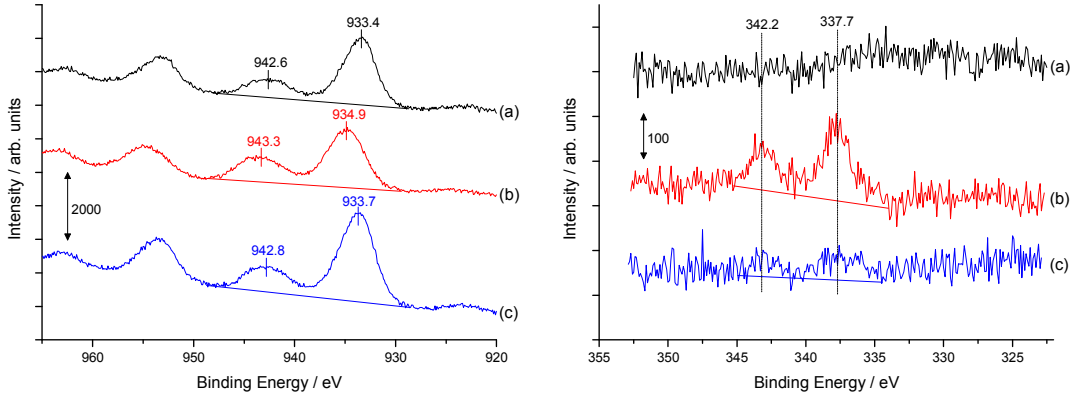

Figure 2 – Cu(2p) and Pd(3d) XP spectra following calcination but before reduction for (a) 10-CI, (b) 50-SI and (c) 50-CP

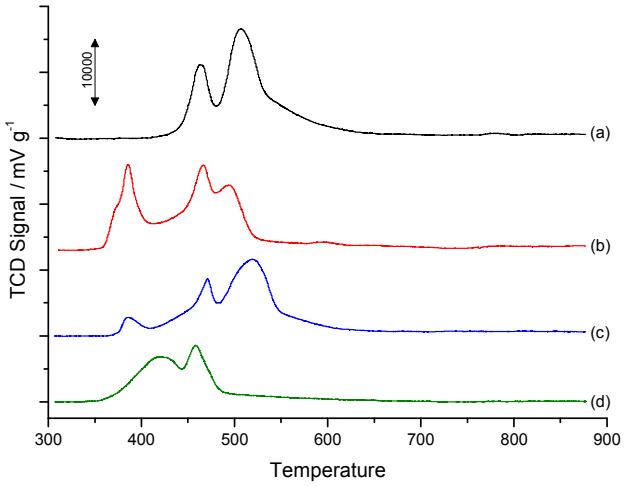

Figure 3 – TPR profiles for (a) 10% Cu/Al_2O_3, (b) 10-CI, (c) 50-SI and (d) 50-CP

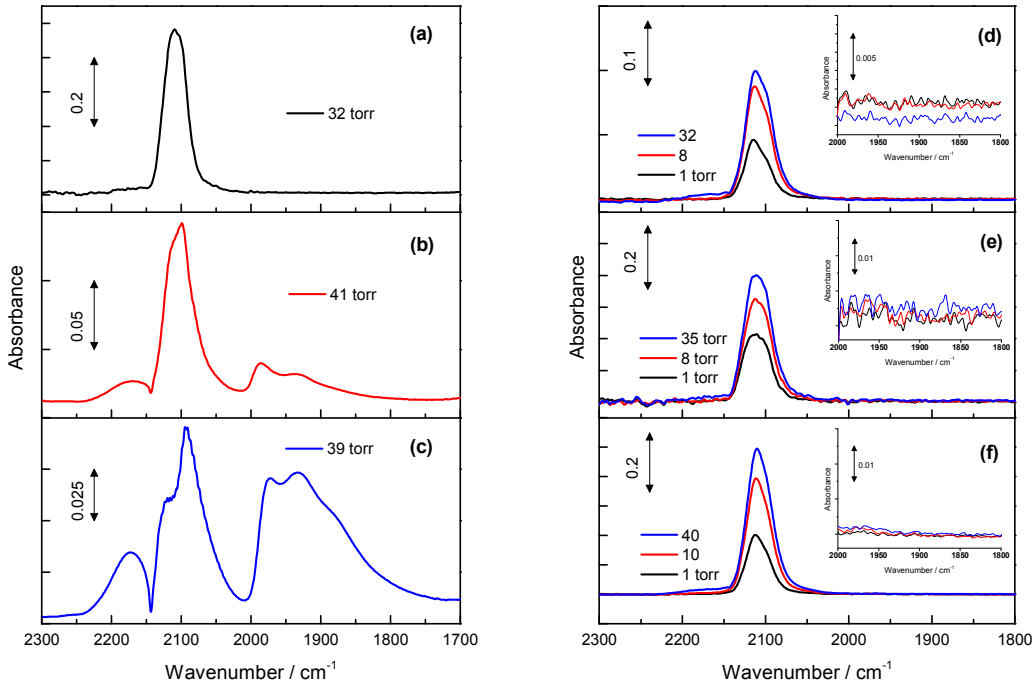

Figure 4 - FTIR spectra of reduced samples after exposure to CO at 298 K. (a) 10% Cu/Al_2O_3, (b) 50:50 physical mixture of 10% Cu/Al_2O_3 and 1.67% Pd/Al_2O_3 (10:1 Cu:Pd ratio), (c) 1.67% Pd/Al_2O_3, (d) 10-CI, (e) 50-SI and (f) 50-CP.

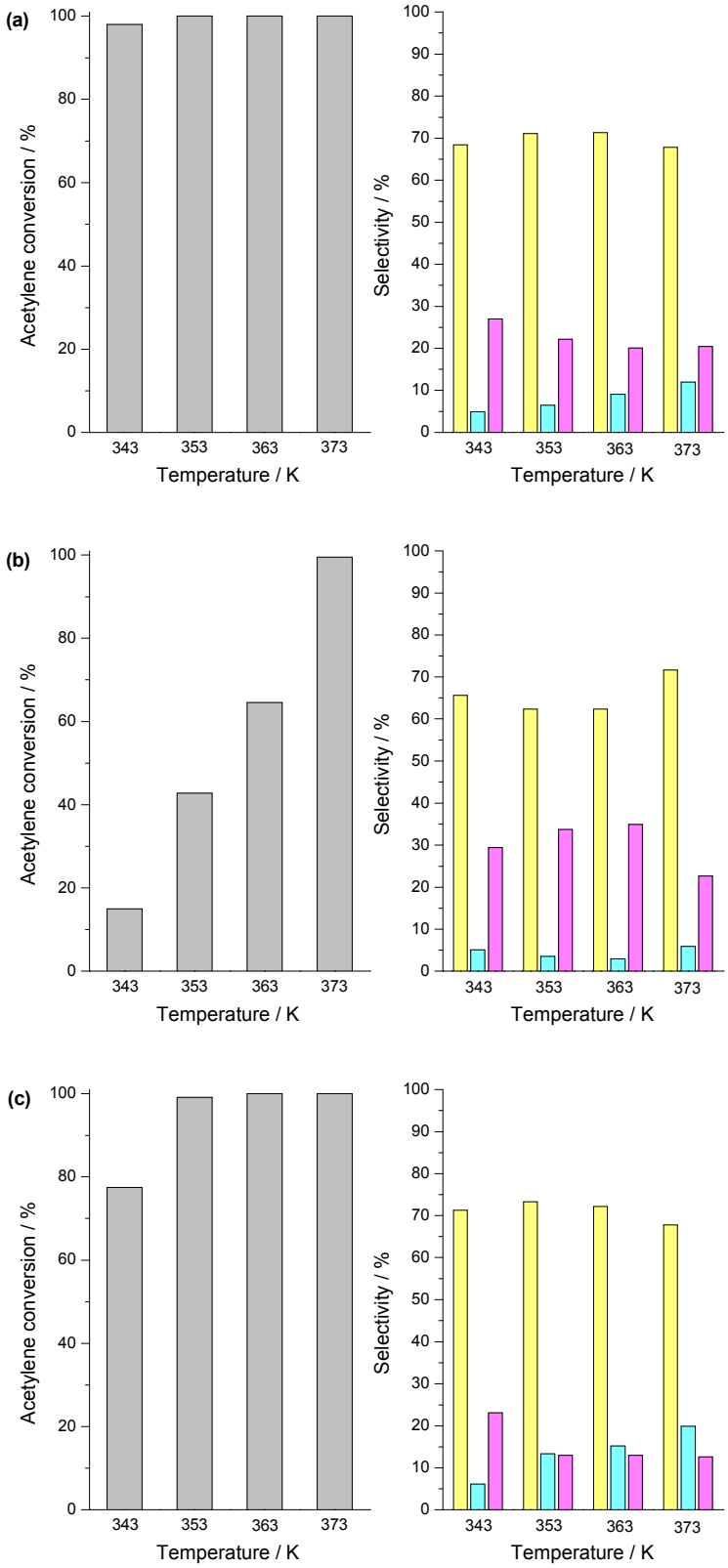

Figure 5 - Acetylene conversion and product selectivity for (a) 10-CI , (b) 50-SI and (c) 50-CP at temperatures between 343-373 K using a 3:1 H_2:acetylene ratio and 1 bar pressure. Acetylene conversion (grey), ethylene selectivity (yellow), ethane (cyan) and oligomer selectivity (pink).

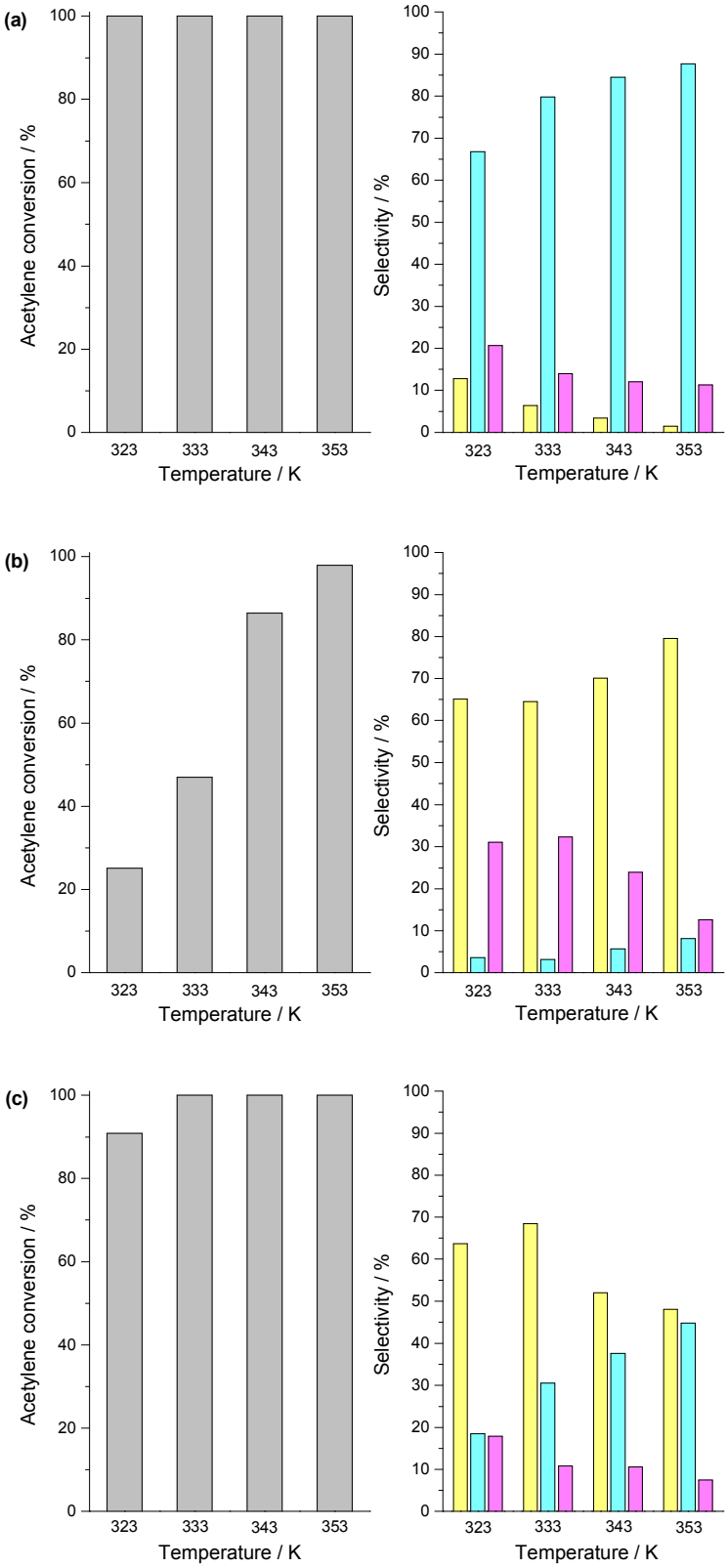

Figure 6 – Acetylene conversion and product selectivity for (a) 10-CI , (b) 50-SI and (c) 50-CP at temperatures between 323-353 K using a 10:1 H_2:acetylene ratio and 1 bar pressure. Acetylene conversion (grey), ethylene selectivity (yellow), ethane (cyan) and oligomer selectivity (pink).

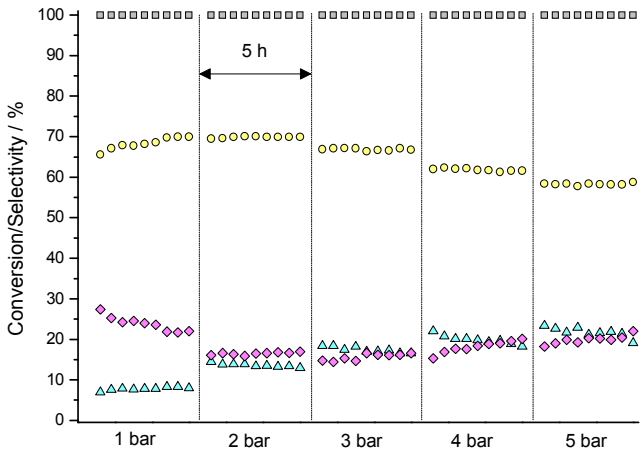

Figure 7 - TOS data for 50-SI at 373 K between 1-5 bar pressure using a 3:1 H_2:acetylene ratio. Acetylene conversion (grey squares), ethylene selectivity (yellow circles), ethane (cyan triangles) and oligomer selectivity (pink diamonds).

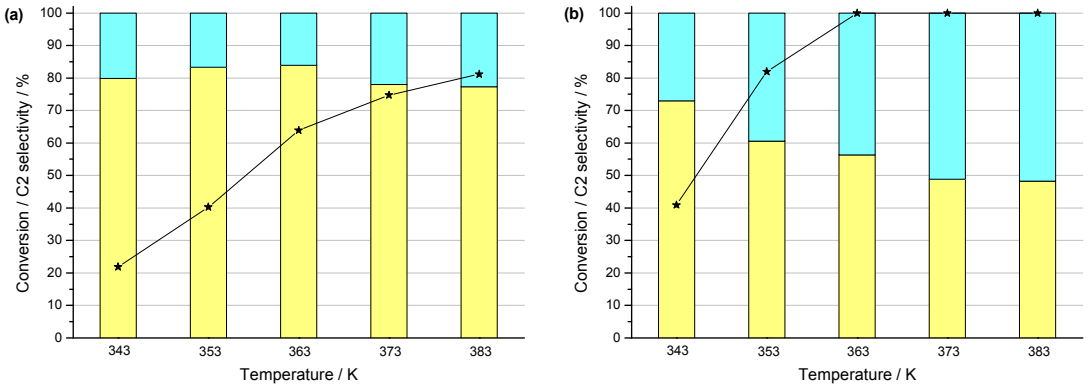

Figure 8 - Acetylene conversion and C2 product selectivity for (a) 50-SI and 1.5:1 H_2:acetylene and (b) 50-SI and 3:1 H_2: acetylene at temperatures between 343-383 K and 1 bar pressure. Acetylene conversion (black stars), ethylene selectivity (yellow bar) and ethane (cyan bar).